chemosensors

Review

Application of Aminopolycarboxylic Complexes of V(IV) in Catalytic Adsorptive Stripping Voltammetry of Germanium

Agnieszka Królicka, Jerzy Zarębski and Andrzej Bobrowski *

Department of Building Materials Technology, Faculty of Materials Science and Ceramics, AGH University of Science and Technology, Mickiewicza 30, 30-059 Krakow, Poland; krolicka@agh.edu.pl (A.K.); zarebski.jerzy@gmail.com (J.Z.)

* Correspondence: abobrow@agh.edu.pl

Abstract: In the review, voltammetric analytical procedures that employ vanadium(IV) and aminopolycarboxylic complexes of V(IV) are presented and discussed. The focus of the paper is on the mechanism of vanadium-catalyzed reactions responsible for the amplification of the analytical signal of Ge(IV). The analytical efficacy of different catalytic systems is compared, and the optimal parameters of the respective procedures are reported.

Keywords: vanadium; germanium; aminopolycarboxylic complexes; catalytic adsorptive stripping voltammetry; HEDTA

check for updates

Citation: Królicka, A.; Zarębski, J.; Bobrowski, A. Application of Aminopolycarboxylic Complexes of V(IV) in Catalytic Adsorptive Stripping Voltammetry of Germanium. *Chemosensors* **2022**, *10*, 36. https://doi.org/10.3390/chemosensors10010036

Academic Editor: Győző G. Láng

Received: 10 November 2021
Accepted: 8 January 2022
Published: 16 January 2022

1. Chemistry and Electrochemistry of Vanadium Compounds

Vanadium is an element with fascinating chemistry and a multitude of applications. The broad application of metallic vanadium and its compounds, as well as its interesting biological properties [1] have been the subject of many research papers and reviews. Its application in catalysis, especially in heterogeneous vanadium catalysis, has been covered in a particularly large number of reviews [2]. Despite the high interest in homogeneous vanadium-catalyzed reactions, few reviews have addressed the catalytic applications of homogeneous vanadium systems [3]. There are also not many reviews devoted to the electrochemical properties of vanadium [4–6]. These properties are unique, since in aqueous solutions vanadium can have up to four oxidation states, i.e., +2, +3, +4, and +5 (Figure 1) [7]. Solid compounds and aqua complexes containing vanadium in various oxidation states differ in color (Figure 1). It is easy to change the oxidation state of vanadium ions (Figure 1), which makes it possible to stage spectacular demonstrations for chemistry students [8], and they are also utilized in all vanadium redox flow batteries, in which the V(II)/V(III), and V(IV)/V(V) couples are used in negative and positive half-cells, respectively [9]. Inorganic compounds of vanadium, such as $VOSO_4$ or V_2O_5, are the most common sources of vanadium in the laboratory owing to their chemical stability, whereas V(III) and V(II) ions are very susceptible to undergoing oxidation to V(IV). In an acidic aqueous solution ($pH < 4$), V(IV) occurs in the form of oxovanadium(IV) ($[VO(H_2O)_5]^{2+}$, VO^{2+}), and as the pH of the solution increases, the $[VO(OH)]^+$ and $[(VO)_2(OH)_2]^{2+}$ ions form. In solutions with $pH > 12$, V(IV) is present in the form of $[VO(OH)_3]^-$ (Figure 1b).

Oxovanadium(IV) ions form numerous complexes with many ligands, resulting in five- or six-membered chelate rings with N or O being the points of attachment (Figure 2, chelate rings marked by the blue ellipse in the image). Detailed descriptions of these chelates, numerous images demonstrating their structure, and an overview of their applications are presented in some recent reviews [10,11]. Examples of vanadium complexes that exhibit biologically significant properties, such as antineoplastic [10,12,13] or insulin-enhancing action [10], are shown in Figure 2.

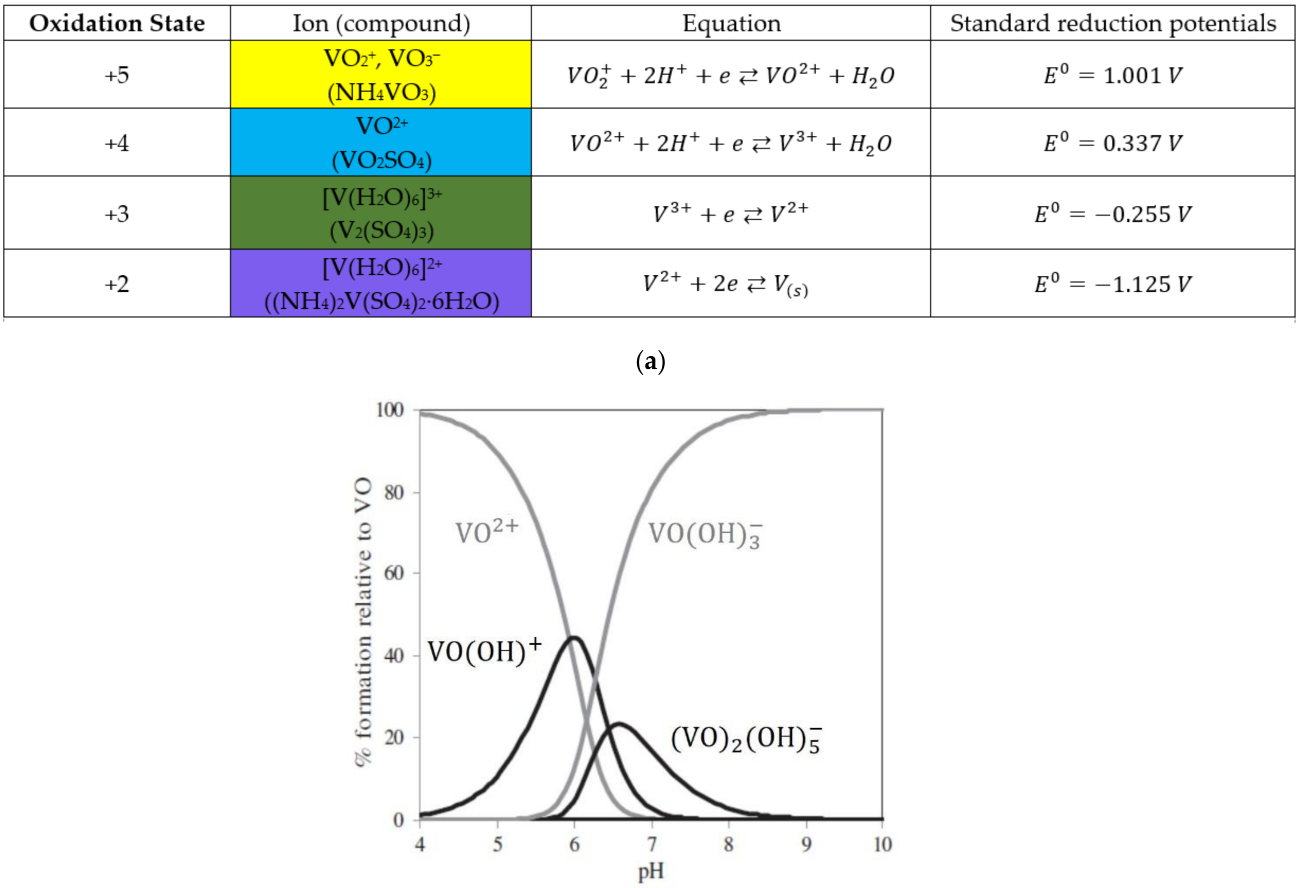

Oxidation State	Ion (compound)	Equation	Standard reduction potentials
+5	VO_2^+, VO_3^- (NH_4VO_3)	$VO_2^+ + 2H^+ + e \rightleftarrows VO^{2+} + H_2O$	$E^0 = 1.001\ V$
+4	VO^{2+} (VO_2SO_4)	$VO^{2+} + 2H^+ + e \rightleftarrows V^{3+} + H_2O$	$E^0 = 0.337\ V$
+3	$[V(H_2O)_6]^{3+}$ ($V_2(SO_4)_3$)	$V^{3+} + e \rightleftarrows V^{2+}$	$E^0 = -0.255\ V$
+2	$[V(H_2O)_6]^{2+}$ ($(NH_4)_2V(SO_4)_2{\cdot}6H_2O$)	$V^{2+} + 2e \rightleftarrows V_{(s)}$	$E^0 = -1.125\ V$

(**a**)

(**b**)

Figure 1. (**a**) oxidation states of vanadium in an aqueous solution, their color and examples of chemical compounds; (**b**) distribution diagram of V(IV) hydrolysis at 10 nM. Reprinted with permission from ref. [10].

Several reports also describe complexes of V(IV) and EDTA, a general-purpose chelating agent most commonly used for laboratory and industrial applications and other more selective aminopolycarboxylates [14–16]. One example of selective complexones is HEDTA (N-hydroxyethyl-ethylene diamine-triacetic acid), whose complexes have found very specific applications (Fe-HEDTA as an active ingredient of low-risk herbicides; Nd(III)-HEDTA and Am(III)-HEDTA in the separation of trivalent actinides from trivalent lanthanides in nuclear fuel cycle research [17,18]). Various structures of EDTA and HEDTA complexes have been described (examples are shown in Figure 2e,f), but there remains much to be discovered with regard to the complexation behaviors of vanadium ions and EDTA-related ligands. Di- or multinuclear vanadium complexes with various types of bridging modes have also been reported [19,20].

The aim of this work was to contribute to our understanding of the use of V(IV) complexes as effective reagents in a homogenous catalytic process employed for the amplification of Ge(IV) analytical signals in voltammetric adsorptive stripping analysis. The results published between 1990 and 2021 were analyzed to elucidate the mechanism of electrochemical processes responsible for the catalytic enhancement of the voltammetric signals of germanium. The formation of a mixed intermediate compound comprising germanium, vanadium, and two ligands is postulated. This hypothesis is supported by the innate ability of vanadium and germanium to form mixed, multinuclear bridged complexes with many ligands. The voltammetric signals would in such a case be amplified as a consequence of the presumed reduction of both Ge(IV) and V(IV) ions bound in the mixed intermediate compound.

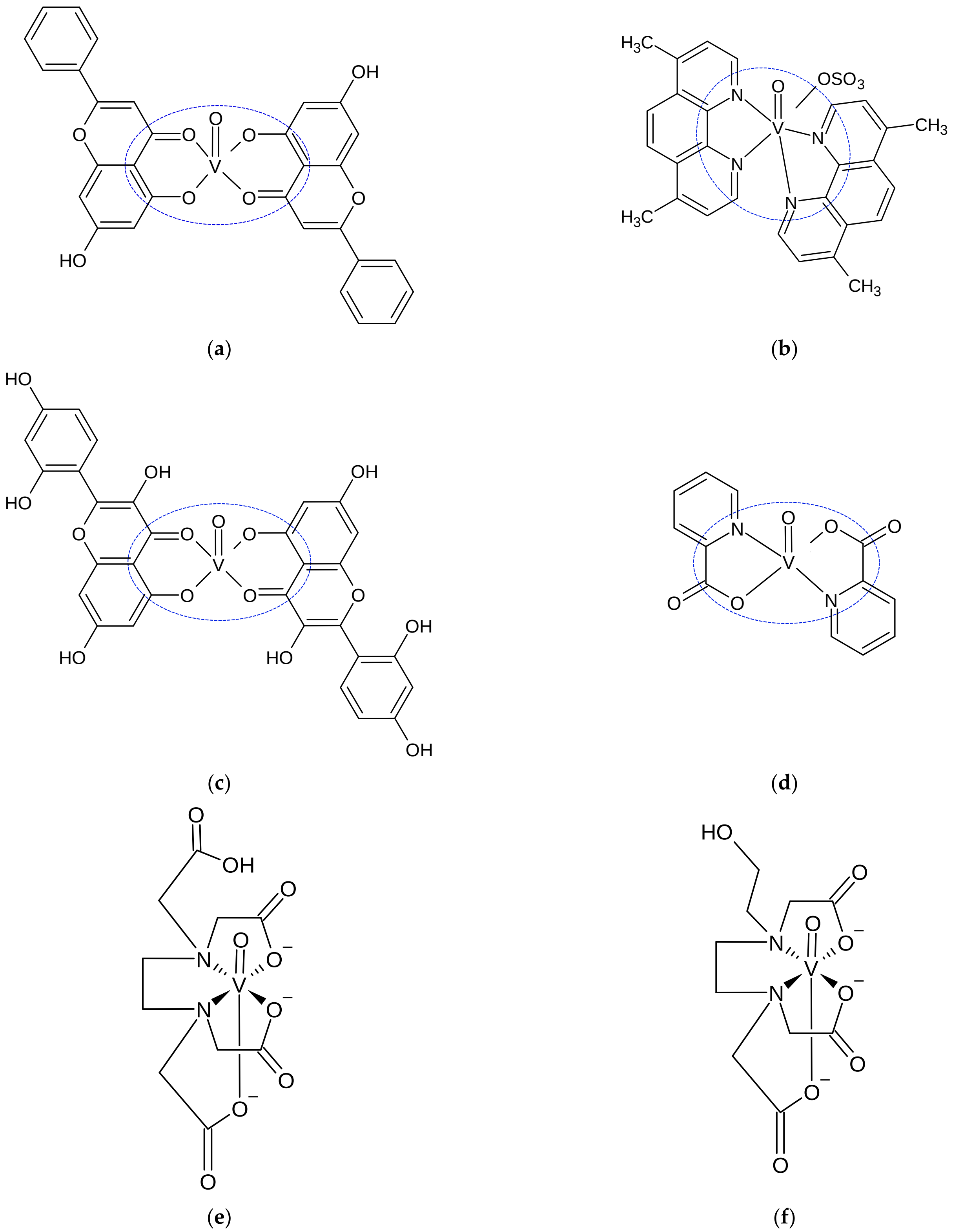

(**a**) (**b**)

(**c**) (**d**)

(**e**) (**f**)

Figure 2. Examples of oxovanadium(IV) complex structures with antineoplastic activity (**a**–**c**) or insulin-enhancing properties (**d**). (**a**) chrysin oxovanadium(IV) complex at physiological pH; (**b**) bis(4,7-dimethyl-1,10-phenanthroline) sulfatooxovanadium(IV) complex (metvan); (**c**) morin oxovanadium(IV) complex; (**d**) picolinic acid oxovanadium(IV) complex. (**e**) V(IV)-EDTA complex; (**f**) V(IV)-HEDTA complex.

2. Adsorptive and Catalytic Adsorptive Stripping Voltammetric Determination of Germanium

2.1. Adsorptive Stripping Voltammetric Determination of Germanium

As can be seen in Figure 3, in organic free aqueous solutions, germanium is present in the form of $Ge(OH)_4$ tetrahydroxide (pH < 7) or as $H_3GeO_4^-$, which dominates in alkaline media (pH > 9) (Figure 3a). In the presence of many ligands containing carboxylic, di-orthophenolic, and polyalcoholic functional groups, Ge(IV) forms stable five-membered ring chelate complexes displaying coordination number 6 (Figure 3b). When only two organic ligands coordinate Ge(IV), the remaining coordination sites are occupied by water molecules [21]. The water molecules can be easily replaced by other ligands and mixed complexes can be formed. Germanium complexes of different 1,2-diphenol derivatives have been used since the 1990s to determine Ge(IV) traces by means of adsorptive stripping voltammetry (AdSV) because of their ability to accumulate on the surface of the working electrode. The AdSV procedures mainly use catechol [22–27], but there are also articles describing how other complexes can also be used to determine trace levels of germanium [28–33].

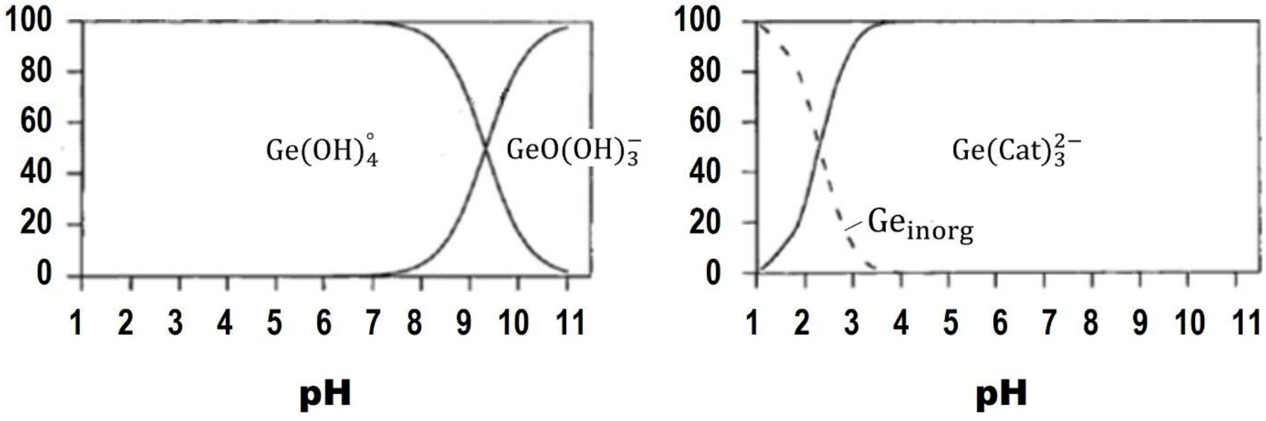

(**a**) (**b**)

Figure 3. Distribution curves of hydroxide complexes of Ge (**a**) and complexes of Ge and catechol (**b**) as a function of pH at 25 °C in aqueous solutions containing 0.02 M of Ge and 0.1 M of catechol. Reprinted with permission from ref. [21].

In recent decades, many researchers have attempted to explain the electrode processes that contribute to the development of the Ge(IV) signal in the presence of catechol and its derivatives, but the results of their research differed significantly. Various electrode reaction schemes have been suggested, but there is no general consensus on the composition and stoichiometry of electroactive complexes [25,26,34] and the nature of products produced by electroreduction processes [25,26,35–38].

When it comes to practical applications, AdSV procedures for the determination of germanium(IV) allow Ge(IV) to be determined at levels of several nanomol per liter [23,25,32]. However, because of the extremely low germanium content in certain samples, a catalytic approach that would provide considerably greater sensitivity would be desirable.

2.2. Catalytic Amplification of Germanium Voltammetric Signals in the Presence of Oxoacid Anions

Anions such as BrO_3^- are among the catalytic agents most widely used for the amplification of voltammetric signals of Ge(IV)-catechol and Ge(IV)-pyrogallol complexes (Table 1). As in the case of AdSV procedures for Ge(IV) determination, several schemes were proposed to describe the catalytic reactions induced by some germanium complexes with ligands containing the -C-(OH)-C-(OH) group (e.g., catechol, gallic acid, pyrogallol) in the presence of various oxidants [35–37,39,40]. These schemes were based on the assumption that the catalytic reaction involves a simple regeneration of the product of electroreduction, namely the Ge(IV)-catechol complex (Scheme 1).

Table 1. Catalytic systems involving germanium and their properties.

Ligand	Catalytic Agent	Supporting Electrolyte	Electrode	P_2/P_1 [1]	Linear Range nM	LOD nM	References
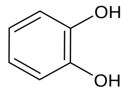 Benzene-1,2-diol catechol	BrO_3^-	Acetate buffer	DME	2.2	1–7000	1	[35]
	VO^{2+}	$HClO_4$, $NaClO_4$	HMDE	11	n.a.	n.a.	[39]
	BrO_3^-	Acetate buffer	HMDE	24	n.a.	n.a.	[40]
	V(IV)-EDTA	Acetate buffer	HMDE	3.5	n.a.	n.a.	[40]
	V(IV)-HEDTA	Acetate buffer	HMDE	26	0.05–20	0.01	[40]
	V(IV)-HEDTA	Acetate buffer	Hg(Ag)FE	n. a.	0.01	0.15	[40]
	V(IV)-HEDTA	Acetate buffer	BiFE/GC	n. a.	1.5–24	1.0	[41]
	V(IV)-HEDTA	Acetate buffer	BiFE/SPE	n. a.	1.5–19.5	1.0	[41]
	V(IV)-HEDTA	Acetate buffer	BiFE/SPE$_{meso}$	n. a.	5.0–70	1.2	[41]
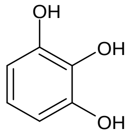 Benzene-1,2,3-triol Pyrogallol	BrO_3^-	Acetate buffer, trisodium citrate	BiFE/GC	1.5	7–230	0.8	[36]
	V(IV)-HEDTA	Acetate buffer	HMDE	100	0.25–25	0.02	[42]
	V(IV)-EDTA	Acetate buffer	HMDE	10	n.a.	n.a.	[42]
	V(IV)-NTA	Acetate buffer	HMDE	1.5	n.a.	n.a.	[42]
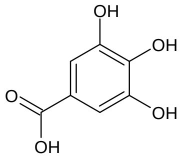 3,4,5-Trihydroxybenzoic acid, gallic acid	V(IV)-EDTA	$HClO_4$	HMDE	n.a.	0.03–10	0.02	[37]
	V(IV)-EDTA	H_2SO_4	DME	10	0.55–275	0.05	[38]
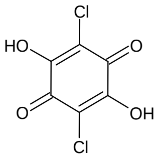 2,5-Dichloro-3,6-dihydroxycyclohexa-2,5-diene-1,4-dione, chloranilic acid	V(IV)-HEDTA	Acetic acid	HMDE	21	0.75–50	0.085	[43]
	V(IV)-HEDTA	Acetic acid	Hg(Ag)FE	12	1–25	0.7	[43]
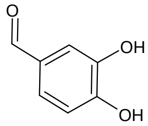 3,4-Dihydroxybenzaldehyde (DHB)	V(IV)-EDTA	KCl	HMDE	17	0.1–10	0.05	[44]

[1] P_2/P_1 amplification factor, i.e., the ratio of peaks shown in Figure 4.

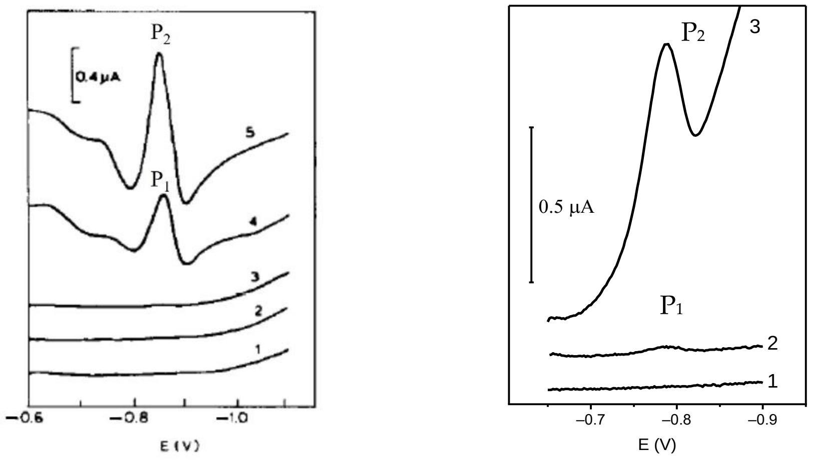

(**a**) (**b**)

Figure 4. (**a**) Linear scan AdSV voltammograms recorded for: (1) 0.07 M acetate buffer (pH 4.6), (2) as in (l) + 0.1 μM of Ge(IV), (3) as in (l) + 1.5 mM catechol, (4) as in (3) + 0.1 μM Ge(IV), (5) as in (4) + 0.1 M $NaBrO_3$, working electrode: DME. Reprinted with permission from ref. [35]; (**b**) DP AdSV voltammograms recorded for: (1) 0.09 M of acetate buffer and 20 nM of Ge, (2) as (l) + 2 mM of catechol, (3) as (2) + 0.014 M of $KBrO_3$; working electrode: HMDE; instrumental parameters $E_{acc} = -0.2$ V, $t_{acc} = 80$ s. Adapted with permission from ref. [40].

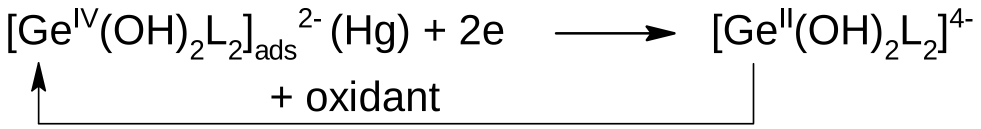

$$[Ge^{IV}(OH)_2L_2]_{ads}^{2-}(Hg) + 2e \longrightarrow [Ge^{II}(OH)_2L_2]^{4-}$$

Scheme 1. Mechanism of the electrode processes responsible for the amplification of the Ge(IV) voltammetric signal in the presence of ligand (L) and oxidant.

According to Scheme 1 the regenerated electroactive ion participates in the electrode process again, contributing to the increase in the number of exchanged electrons and, eventually, to the increase in analyte peak currents.

The ratio of the peak current obtained when the catalytic system is used to the peak current obtained for the AdSV system in the absence of an oxidant ranges from several to several dozen. The amplification factor (P_2/P_1) depends on many parameters, primarily on the type of oxidant and ligand that form complexes with Ge(IV), but also on the type of the working electrode, the supporting electrolyte composition, and the instrumental parameters. For example, Figure 4 highlights the difference the Ge(IV) signals obtained with a dropping mercury electrode (DME) and a hanging mercury drop one (HMDE). The P_2/P_1 ratio, where P_2 represents the catalytic signal and P_1 the AdSV signal, amounted only to 2.2 in the case of the voltammograms recorded using DME (Figure 4a), but it was as high as 28 when the HMDE was used (Figure 4b).

2.3. Catalytic Amplification of Germanium Voltammetric Signals in the Presence of Free Oxovanadium(IV) Ions

As shown in Figure 5 (curve d), the germanium peak produced in a solution containing 1 mM of $HClO_4$, 0.1 M of $NaClO_4$, 0.01 mM of catechol, and 0.2 mM of Ge(IV) is well-developed, symmetrical, but not pronounced. After the addition of 2mM of $VOSO_4$ to the supporting electrolyte, the recorded peak current of Ge(IV) is 11 times higher. This increase may be attributed to a catalytic effect. In a solution containing catechol and VO^{2+} ions, the latter can be complexed with catechol (Scheme 2), but most of the vanadium content is present in the form of free VO^{2+} ions. These free ions thus participate in the catalytical reaction [39].

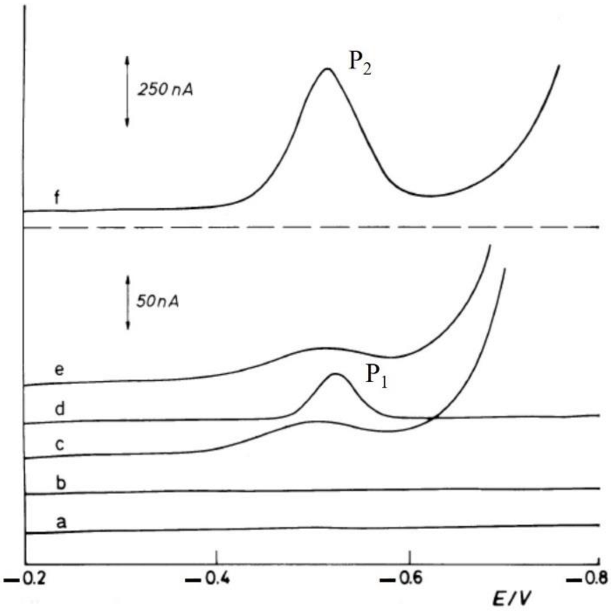

Figure 5. DP voltammograms recorded in a solution containing 1 mM of $HClO_4$ + 0.1 M of $NaClO_4$ (pH 2.9) and: (a) 0.2 mM of Ge(IV); (b) 0.01 mM of catechol; (c) 2 mM of V(IV); (d) 0.01 mM of catechol + 0.2 mM of Ge(IV) (P_1); (e) 0.01 mM of catechol + 3 mM of V(IV); (f) 2 μM of catechol + 0.2 mM of Ge(IV) + 3 mM of V(IV) (P_2). $E_{acc} = -0.2$ V; t_{acc} = 5s. Reprinted with permission from ref. [39].

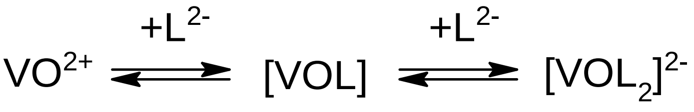

L^{2-}—catechol anion

Scheme 2. Oxovanadium(IV) complexes of catechol (L) in aqueous solution.

2.4. Catalytic Amplification of Germanium Voltammetric Signals in the Presence of V(IV)-EDTA

A study by Sun [44] suggested for the first time that the V(IV)-EDTA complex can be applied to amplify the adsorptive stripping voltammetric signal obtained for the Ge(IV)-3,4-dihydroxybenzaldehyde (DHB) complex. In this case, the amplification factor expressed as the P_2/P_1 peak current ratio (Figure 10a) was equal to 17. The authors [44] also tested other reagents with the potential to induce catalytic effects, such as $HClO_4$ and $NaClO_4$, but these reagents did not produce the desired amplification. Eventually, a solution (pH 2.0–2.5) containing 0.1 M of KCl, 2 mM of EDTA, 1 mM of DHB, and 3mM of V(IV) was found to be most beneficial.

The peak current of Ge(IV) was linear over the concentration range of 0.1–10 nM (LOD = 0.05 nM, $E_{acc} = -0.05$ V, t_{acc} = 60 s). In [44], the authors claimed that the amplification of the Ge(IV) signal is caused by the reoxidation of the product obtained by the electroreduction reaction, described by Scheme 3. They did not explain the role of EDTA [44].

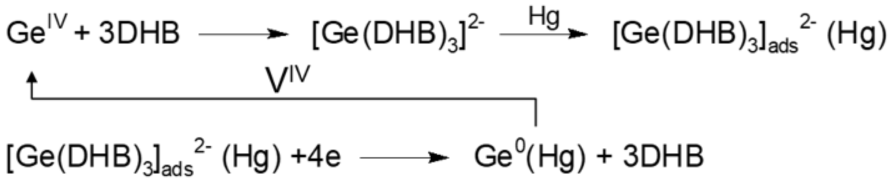

Scheme 3. Mechanism of the electrode processes responsible for the amplification of the Ge(IV) voltammetric signal in the presence of 3,4-dihydroxybenzaldehyde (DHB) and V^{IV}.

The influence of the concentration of V(IV) and EDTA on the signal of Ge(IV) complexed by gallic acid was studied in a detail by Li [37]. The published data confirmed that EDTA plays a significant role in the catalytic system of Ge(IV)-gallic acid-V(IV). Initially, the current response of the Ge(IV)-gallic acid-V(IV) system increased with EDTA concentration, and it then reached a plateau at 3.0–4.2 mM of EDTA, showing that the concentration of EDTA must be at least equal to that of V(IV) to effectively amplify the signal produced by this catalytic system. Assuming the Ge(IV)-gallic acid complex to be stoichiometric, Li et al. [37] presented the possible mechanism of electrode processes (Scheme 4). According to this scheme, Ge(IV) ions form a complex with gallic acid, which is subsequently adsorbed on the mercury drop electrode. When potential is applied in the negative direction, the Ge(IV) in the complex is reduced to Ge(II), which is then chemically oxidized to Ge(IV) by V(IV)-EDTA. The reoxidized Ge(IV) complexed with gallic acid once again participates in the electrode process and contributes to the reduction current [37].

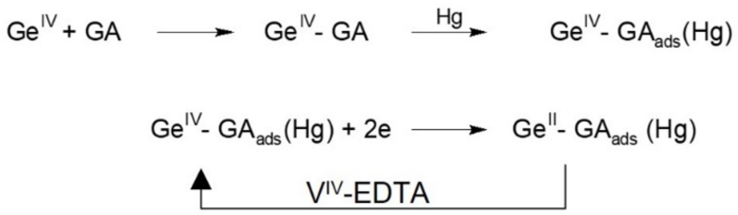

Scheme 4. Mechanism of the electrode processes responsible for the amplification of the Ge(IV) voltammetric signal in the presence of gallic acid and V^{IV}-EDTA.

The optimal supporting electrolyte recommended for the determination of Ge(IV) contains 0.03 M of $HClO_4$ (pH 1.6, 6.0 mM of gallic acid, 3.0 mM of V(IV) and 4.0 mM of EDTA) [37]. The Ge (IV) peak current was linear over the concentration range of 0.03–10 nM (LOD = 0.02 nM, $E_{acc} = -0.1$ V, $t_{acc} = 120$ s).

The influence of V(IV) and EDTA on the germanium signal was also examined for the Ge (IV) catecholate complex [40]. The catalytic amplification factor was estimated to be 3.5 (Figure 4b).

2.5. Catalytic Amplification of Germanium Voltammetric Signals in the Presence of V(IV)—HEDTA

2.5.1. Determination of Germanium Using Hanging Mercury DROP Electrode

When EDTA in the Ge(IV)-catechol-V(IV)-EDTA system was substituted with HEDTA, a marked enhancement of germanium signals was observed. The catalytic amplification factor amounted to 26 for HEDTA (Figure 10c) and only 3.5 for EDTA (Figure 10b). Although the catalytic enhancement of the Ge signal in the case of HEDTA was comparable to that obtained with BrO_3^-, for which the catalytic amplification was equal to 24, the signal produced in the presence of bromide is analytically less useful due to a significant overlap of the reduction current of the oxidant and the subsequent asymmetry of the catalytic curve [40].

To explain the role of V(IV) and HEDTA in the catalytic-adsorptive system comprising the Ge (IV)-catechol complex, detailed voltammetric studies were performed [40]. As shown in Figure 6, the voltammogram recorded in the solution containing 10 nM of Ge and 1 mM of catechol presents a weak but measurable signal P_1* at a potential of −0.780 V, representing the reduction of the adsorbed Ge(IV)-catechol complex. After the addition of 1 mM of V(IV) to the investigated solution, a new peak (P_2) appeared at a potential of −0.914 V, originating from the reduction of the newly formed V(IV)-catechol complex. The addition of one more reagent, i.e., 0.25 mM of HEDTA, resulted in the appearance of another signal at a potential of −1.1 V, originating from the reduction of V(IV) ions in the V(IV)-HEDTA complex. The previously observed reduction peak of Ge (IV) (P_1*) was no longer observed until the HEDTA concentration exceeded 1.0 mM. When the HEDTA concentration reached 1 mM, the germanium peak reappeared. Moreover, it was significantly enhanced (compare P_1* and P_1). It was evident that the enhanced germanium peak (P_1) appeared when the molar ratio of HEDTA to V(IV)/ratio was greater than 1 [40]. The observed interdependence between Ge(IV), V(IV), catechol, and HEDTA indicates that the catalytic reaction did not just involve a simple regeneration of the adsorbed product of electroreduction, but was considerably more complex. It is most likely that the catalytic reactions responsible for the amplification of the Ge(IV) voltammetric signal are catalytic processes of the second kind, discussed in previous papers [45–48].

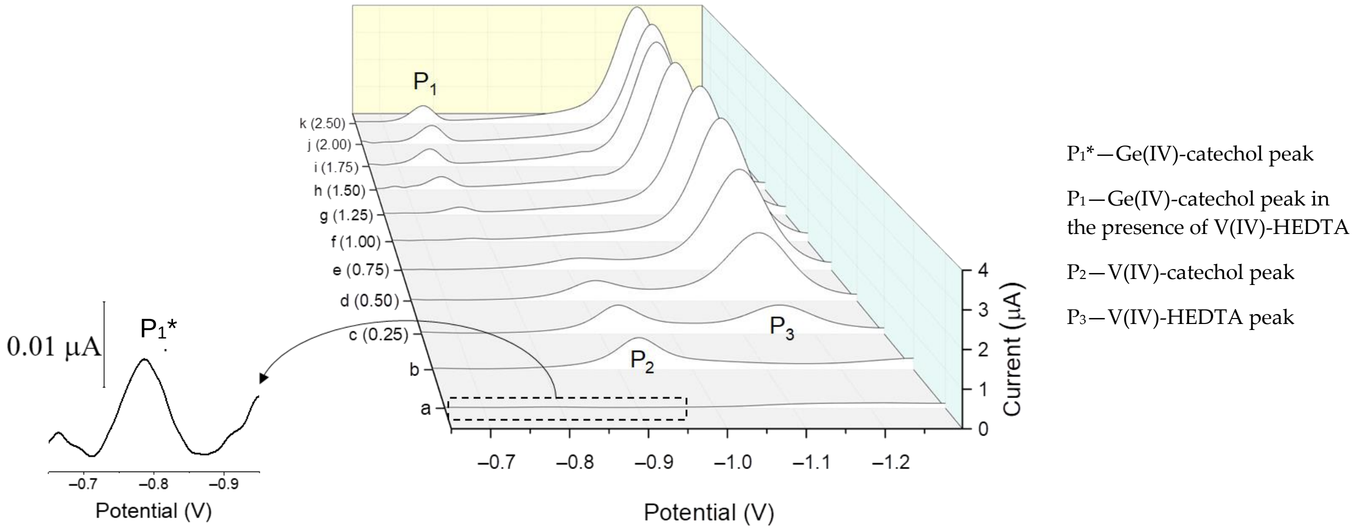

Figure 6. DP-AdSV voltammograms recorded in a solution containing: (a) 10 nM of Ge and 1mM of catechol, (b) 10 nM of Ge, 1 mM of catechol and 1 mM of V(IV). Voltammograms (c–k) were recorded for solution (b) spiked with increasing amounts of a 0.2 M solution of HEDTA in order to obtain the following final concentrations of HEDTA: (c) 0.25 mM, (d) 0.5 mM, (e) 0.75 mM, (f) 1.0 mM, (g) 1.25 mM, (h) 1.5 mM, (i) 1.75 mM, (j) 2.0 mM and (k) 2.50 mM. The values provided in brackets represent the V(IV)/HEDTA ratio. Supporting electrolyte: 0.05 M acetate buffer (pH = 4.4). Instrumental parameters: E_{acc} = −0.2 V, t_{acc} = 80 s. Reprinted with permission from ref. [40].

Under this assumption, the electroreduction of adsorbed Ge(IV)-catechol produces a very active Ge(II)-catechol complex (Scheme 5), which forms a composite complex with V(IV)-HEDTA denoted as (Scheme 5). In this composite complex, vanadium(IV) undergoes reduction to vanadium(II), which results in the breakdown of the multicomponent complex. The regenerated germanium catecholate complex retains its activity (Scheme 5) and combines with additional V(IV)-HEDTA ion. In this way, the catalytic cycle forms, indicated by an arrow in Scheme 5. The number of electrons per germanium ion exchanged during electroreduction increases significantly, which contributes to a substantial rise in the current of the recorded germanium peaks, and thus to an increase in the sensitivity of the analytical procedure.

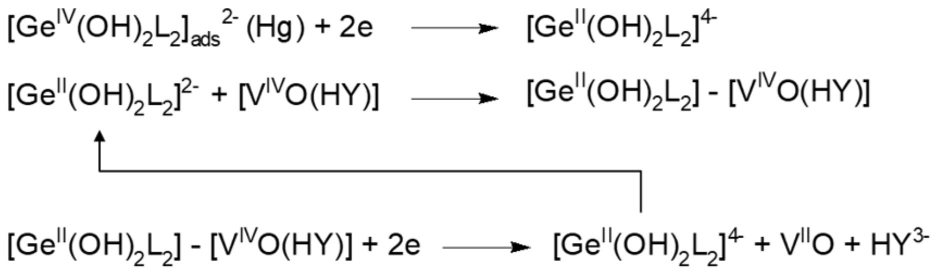

Scheme 5. Catalytic reactions responsible for the amplification of the Ge(IV) voltammetric signal.

The V(IV)-EDTA-induced catalytic processes are likely to follow the same mechanism as V(IV)-HEDTA. The difference in the catalytic efficacy of V(IV)-EDTA (amplification factor 3.5, Table 1) or V(IV)-HEDTA (amplification factor 26, Table 1) can be attributed to their different capacities to form composite complexes with Ge(II)-catechol. Additionally, as determined from cyclic voltammograms, the reduction of the V(IV)-HEDTA complex requires a lower activation energy than that of V(IV)-EDTA, and V(IV) can react with the reduced form of the germanium catechol complex (Ge(II)-catechol) more effectively [40,42].

The recommended supporting electrolyte for the determination of Ge(IV) contained 0.05 M of acetate buffer (pH 4.4), 1 mM of catechol, 1 mM of V(IV), and 1.5 mM of HEDTA. When the HMDE was used, the catalytic response was linear over the range of 0.05–20 nM Ge(IV) (LOD = 0.01 nM, $E_{acc} = -0.2$ V, $t_{acc} = 80$ s).

In addition to catechol, other Ge(IV)-complexing ligands containing an ortho-dihydroxybenzene moiety were also tested in combination with V(IV)-HEDTA to develop catalytic systems. The complex of Ge(IV) with gallic acid produced both AdSV and CAdSV peaks, but its CAdSV signal was four times lower than that observed when pyrogallol was used as a ligand complexing Ge(IV). The amplification factor for the Ge(IV)-pyrogallol-V(IV)-HEDTA system was as high as 100 (Figure 11). It was found that the optimal composition of the supporting electrolyte that guarantees the high sensitivity of the determination using the Ge(IV)-pyrogallol-V(IV)-HEDTA catalytic system contained 0.05 M of acetate buffer (pH 4.5–4.6), 1 mM of pyrogallol, 2 mM of V(IV), and 4 mM of HEDTA.

Chloranilic acid was also investigated as a Ge(IV)-complexing agent [43]. As shown in Figure 7a, the introduction of V(IV)-HEDTA to the solution composed of 0.1 M of acetic acid, 0.5 mM of chloranilic acid, and 1.5 mM of V(IV) led to a significant increase in the Ge(IV) peak current (P_2/P_1 ratio was 21). Furthermore, the investigated Ge(IV) -chloranilic acid-V(IV)-HEDTA system exhibited an interesting dependence of the germanium peak current on the accumulation potential and time, since the actual ligand capable of complexing Ge (IV), 2,5-dichloro-1,3,4,6-tetrahydroxy-benzene (THDB), was produced via the electroreduction of chloranilic acid during the preconcentration step. The cyclic voltammograms of chloranilic acid and the corresponding scheme describing the reduction of chloranilic acid to THDB are shown in Figure 8 [43].

The results of cyclic voltammetric studies indicated that the catalytic amplification of the signal originating from the Ge(IV)-chloranilic acid complex observed in the presence of V(IV)-HEDTA is typical of catalytic systems of the second kind. This entails the formation of the composite complex as an intermediate product (L represents THDB and HY—HEDTA). The optimal supporting electrolyte consisted of 0.1 M of CH_3COOH (pH 2), 0.75 mM of chloranilic acid, and 2 mM of V(IV)-HEDTA. The accumulation was carried out at −0.1 V for 60 s. The germanium signal increased linearly with Ge(IV) concentration over the range of 0.75–50 nM (LOD = 0.085 nM) [43].

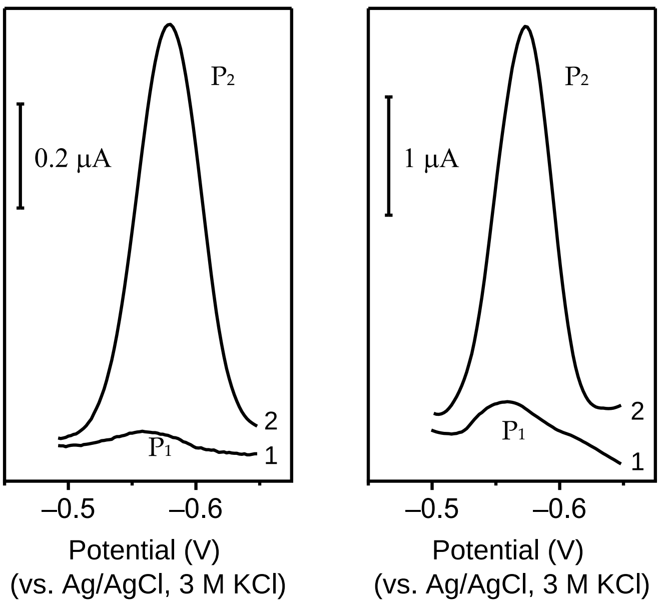

(**a**) (**b**)

Figure 7. DP AdSV curves recorded for a solution containing 25 nM of Ge (IV) and chloranilic acid, in the absence (curve 1) and presence of V(IV)-HEDTA (curve 2) using the HMDE (**a**) and Hg(Ag)FE (**b**). Supporting electrolyte: (**a**) 0.1 M of acetic acid, 0.5 mM of chloranilic acid, 1.5 mM of V(IV), 3 mM of HEDTA; (**b**) 0.075 M of acetic acid, 0.77 mM of chloranilic acid, 1 mM of V(IV), 2 mM of HEDTA. Instrumental parameters: $E_{\mathrm{acc}} = -0.1$ V, $t_{\mathrm{acc}} = 60$ s Reprinted with permission from ref. [43].

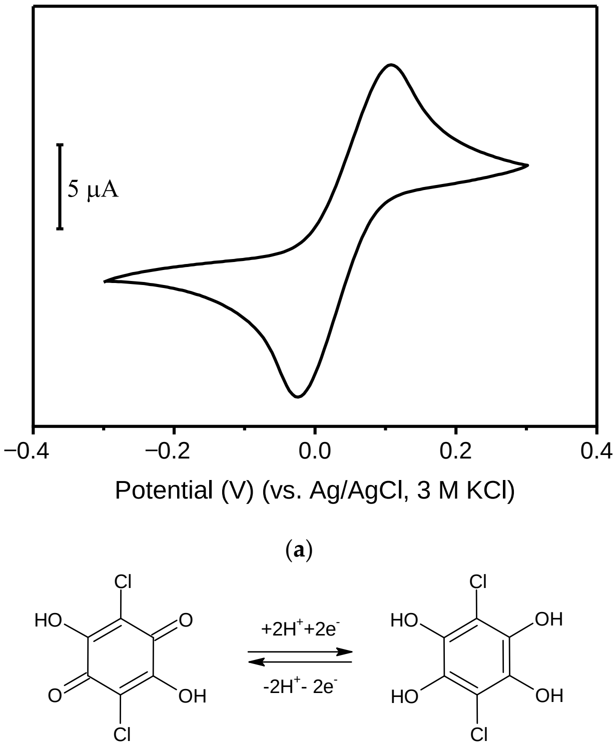

(**a**)

(**b**)

Figure 8. (**a**) CV voltammograms recorded for a solution containing 0.5 mM of chloranilic acid and 0.1 M of acetic acid using a glassy carbon electrode (d = 3 mm). Scan rate: 50 $\mathrm{mVs^{-1}}$. (**b**) Electroreduction of chloranilic acid.

2.5.2. Determination of Germanium Using the Silver Amalgam Film Electrode

Non-toxic working electrodes, such as the silver amalgam film electrode (Hg(Ag)FE) (Figures 8b and 9a) and a family of bismuth-plated electrodes (Section 2.5.3) [41], were also tested. Both Ge(IV)-catechol (Figure 8b) and Ge(IV)-chloranilic acid (Figure 9a) catalytic systems of V(IV)-HEDTA produced well-developed signals of germanium. The optimal composition of the supporting electrolyte differed slightly, as acetate buffer and acetic acid were used for systems based on Ge(IV)-catechol and Ge(IV)-chloranilic acid, respectively. The germanium signal increased linearly with Ge(IV) concentration over the range of 0.2–10 nM (LOD = 0.15 nM) for Ge(IV)-catechol and over 1–25 nM (LOD = 0.70 nM) when the system with chloranilic acid system was used. Both systems were successfully applied for the determination of germanium in mineral water [40,43].

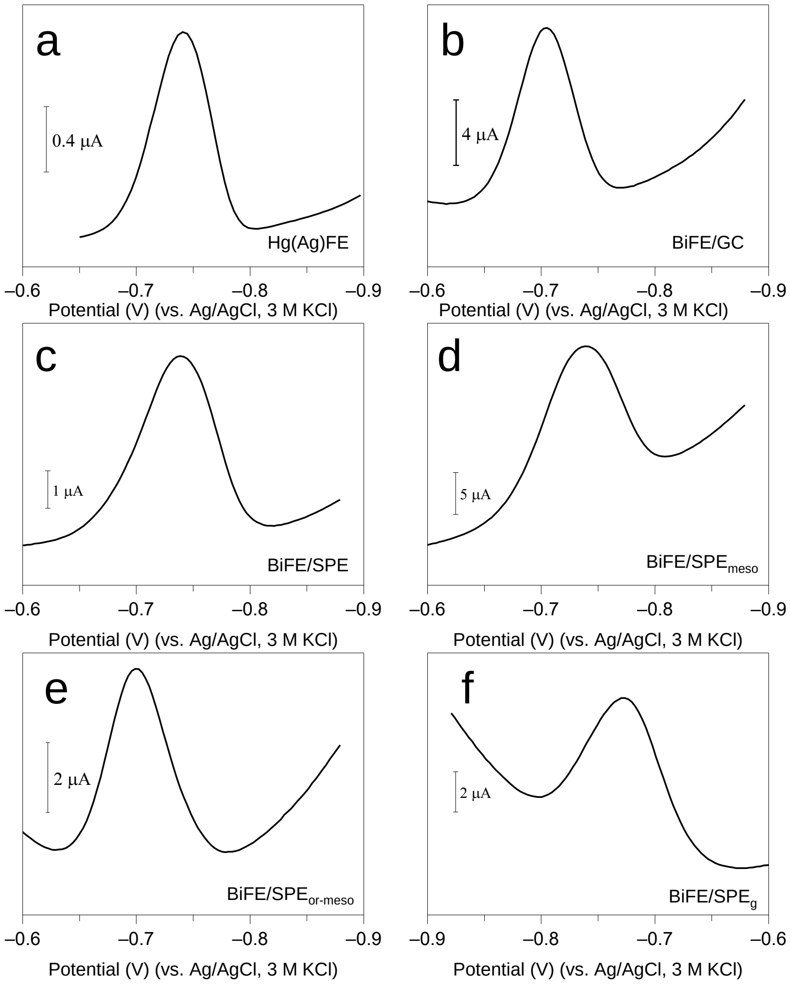

Figure 9. DP AdSV voltammograms recorded for solutions containing for 10 nM of Ge(IV) (**a**) (Hg(Ag)FE only) and (**b**–**f**) 30 nM of Ge(IV)—using bismuth films plated on (**b**) GC (BiFE/GC), (**c**) carbon SPE (BiFE/SPE), (**d**) mesoporous carbon SPE (BiFE/SPE$_{meso}$), (**e**) ordered mesoporous carbon SPE (BiFE/SPE$_{or\text{-}meso}$), (**f**) and graphene SPE (BiFE/SPE$_{g}$). Composition of the supporting electrolyte: 0.05 M of acetate buffer, 1 mM of catechol, 1 mM of V(IV) and 1.5 mM of HEDTA. Instrumental parameters: $E_{acc} = -0.2$ V (Hg(Ag)FE) or $E_{acc} = -0.4$ V (BiFEs), $t_{acc} = 80$ s (Hg(Ag)FE) or $t_{acc} = 30$ s (BiFEs). Bismuth film electrode preparation: electrodeposition at -0.9 V in a 0.04 M Bi(III) solution, carried out for a period sufficient to transfer a charge of 7.07 mC per mm^2 of the surface area of the support electrode [41].

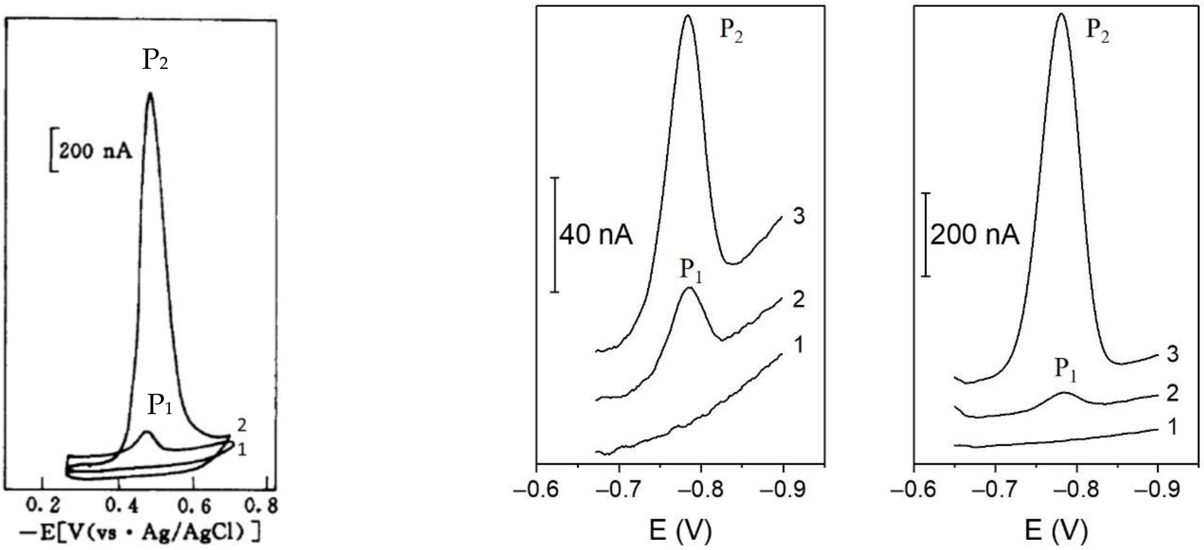

(**a**) (**b**) (**c**)

Figure 10. (**a**) CV voltammograms recorded for: (1) 0.1 M of KCl, 1 mM of DHB, 2 mM of EDTA and 10 nM of Ge(IV) (pH = 2.2) (1), (2)—as for (1), but with an additional 3mM of V(IV). Instrumental parameters: scan rate = 100 mVs^{-1}, E_{acc} = −0.25 V, t_{acc} = 30 s. Reprinted from [42] with permission from Elsevier. (**b**) DP voltammograms of (1) 0.05 M of acetate buffer and 20 nM of Ge, (2)—as for (1), but with the addition of 1.0 mM of catechol, (3)—as for (2), but with the addition of 1 mM of V(IV) and 1.5 mM of EDTA. Instrumental parameters: E_{acc} = −0.2 V, t_{acc} = 80 s [40]. (**c**) DP voltammograms of (1) 0.05 M of acetate buffer and 20 nM of Ge, (2)—as for (1), but with the addition of 1.5 mM of catechol, (3)—as for (2), but with the addition of 1mM of V(IV) and 1.5 mM of HEDTA. Instrumental parameters: E_{acc} = −0.2 V, t_{acc} = 80 s. Adapted with permission from ref. [40].

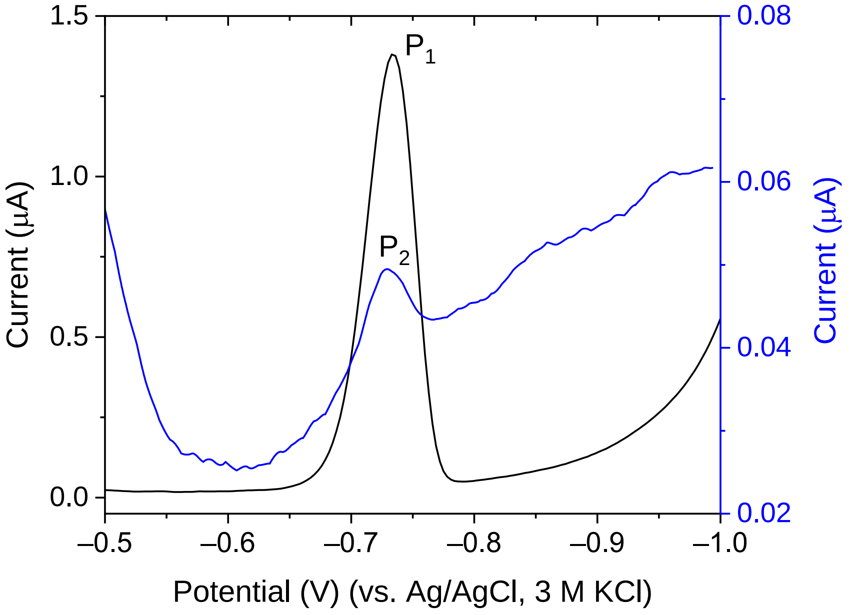

Figure 11. DP AdSV voltammograms recorded for: (1) 0.05 M acetate buffer containing 1 mM of pyrogallol and 15 nM of Ge(IV), (2)—as for (1) but with the addition of 1 mM of V(IV) and 2 mM of HEDTA. E_{acc} = −0.1 V, t_{acc} = 60 s Reprinted with permission from ref. [42]. Copyright 2020 John Wiley and Sons.

2.5.3. Determination of Germanium Using Bismuth Film Electrodes

Experiments with bismuth film electrodes (Figure 9b–f), especially those plated on screen-printed supports, demonstrated the extraordinary ability of V(IV)-HEDTA as an oxidant in catalytic systems involving Ge(IV). Other oxidants, such as nitrite, nitrate, bromate, and chlorate, usually prevent the application of screen-printed electrodes as working electrodes in catalytic stripping voltammetry due to the insufficient resistance of the binders to the action of these chemicals, which often causes the integrity and adhesion of the printed layers to become progressively worse [49]. Both the bismuth layer and the screen-printed supports seemed to be stable and retained their electrochemical activity when exposed to the solution containing the V(IV)-HEDTA complex. The stability of bismuth deposits was confirmed by means of microscopic inspection as well as voltammetric and contact angle measurements [41]. The dependence of the germanium peak current on the concentration of Ge(IV) ions examined in a solution containing 0.05 M of acetate buffer, 1 mM of catechol, 1 mM of V(IV), and 1.5 mM of HEDTA with 30 s of adsorptive accumulation at -0.4 V was linear over the range of 1.5–24 nM for BiFE/GC, 1.5–19.5 nM for BiFE/SPE, 5.0–70 nM for BiFE/SPE$_{\text{meso}}$, and 5.0–90 nM for BiFE/SPE$_{\text{or-meso}}$ [41]. The LOD values ranged from 0.8 nM for BiFE/SPE$_{\text{or-meso}}$ and 1.2 nM for BiFE/SPE$_{\text{meso}}$.

2.6. Catalytic Amplification of Germanium Voltammetric Signals by Other Aminopolycarboxylic Acid Complexes with V(IV)

For a better understanding of the catalytic properties of V(IV) complexes, the experiments were extended to include two additional aminopolycarboxylic acids, such as NTA and DHPTA (Figure 3c,d). Studies showed that both chelating agents are capable of complexing V(IV), as demonstrated by the changing color of the V(IV) solution after the addition of NTA and DHPTA (Figure 12a) and the results of voltammetric studies (Figure 12b). Cyclic voltammograms had well-developed peaks related to the reduction and oxidation of vanadium complexes with the tested chelating agents (Figure 12b). Furthermore, it was found that the intensity of the germanium signal clearly correlates with the voltammetric signal representing the V(IV)/V(II) redox couple. The catalytic activity of different V(IV) complexes was related to the reversibility of the electrode processes of vanadium reduction. The measure of reversibility was the separation of the cathodic and anodic peak potentials recorded via the CV method, expressed by ΔE_{p} in Figure 12c. A vanadium complex that undergoes a more electrochemically reversible reduction can amplify the germanium signal to a greater extent than the one that is reduced irreversibly. For example, in the case of V(IV)-HEDTA, peak-to-peak separation amounts to 0.06 V and the amplification factor for germanium is equal to 100, while for V(IV)-NTA the peak-to-peak separation is as high as 0.31 V and the amplification factor is only 1.5 (Figure 12c). Overall, these results indicate that a simple cyclic voltammetric test can be used to select the most promising candidates for V(IV) chelating agents in catalytic adsorptive stripping voltammetry.

2.7. New Catalytic Systems Comprising Ge(IV) Complexes and V(IV)-HEDTA

To validate the hypothesis that the voltametric signals of Ge(IV) ions complexed by catechol derivatives can be significantly amplified in the presence of aminopolycarboxylic acid complexes of V(IV), we tested three new ligands, namely catechin, sodium alizarin monosulfonate, and alizarin complexone.

When added to acetate buffer comprising 50 µM Ge(IV), all tested complexes delivered measurable AdSV signals at potentials of -0.645 V for catechin, -0.637 V for alizarin sodium monosulfonate, and -0.655 V for alizarin complexone. After the addition of V(IV)-HEDTA, the Ge(IV) peak current was amplified, and peaks were shifted toward more positive potentials. The extent of the changes depended on the concentration of V(IV)-HEDTA, as shown in Figure 13.

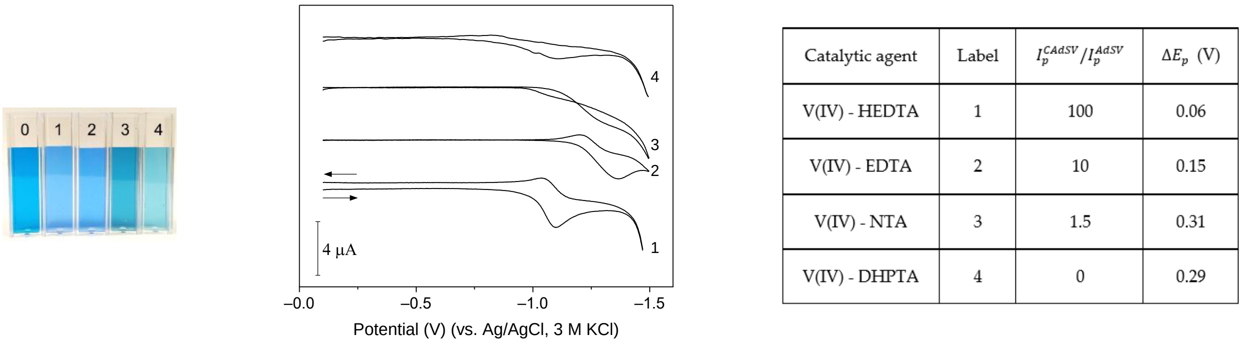

Catalytic agent	Label	I_p^{CAdSV}/I_p^{AdSV}	ΔE_p (V)
V(IV) - HEDTA	1	100	0.06
V(IV) - EDTA	2	10	0.15
V(IV) - NTA	3	1.5	0.31
V(IV) - DHPTA	4	0	0.29

(**a**) (**b**) (**c**)

Figure 12. (**a**) Solutions containing 1 mM of V(IV) (0), 1 mM of V(IV) and 2 mM of HEDTA (1), 1 mM of V(IV) and 2 mM of EDTA (2), 1 mM of V(IV) and 2 mM of NTA (3) and 1 mM of V(IV) and 2 mM of DHPTA (4) in polystyrene cuvettes. (**b**) CV voltammograms recorded in 0.05 M acetate buffer containing 1 mM of V(IV) and 2 mM of HEDTA (1), 2 mM of EDTA (2), 2 mM of NTA (3) or 2 mM of DHPTA (4); scan rate = 50 mVs^{-1}; (**c**) Amplification factors measured for Ge(IV) signals obtained using different catalytic agents and the corresponding peak-to-peak separation (ΔE_p) of the vanadium redox couple. Reprinted with permission from ref. [42]. Copyright 2020 John Wiley and Sons.

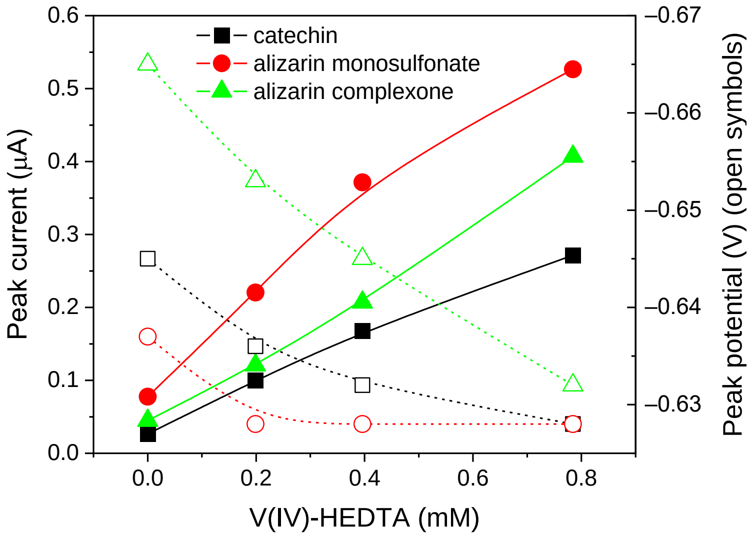

Figure 13. The influence of V(IV)-HEDTA concentration on DP peak current and peak potential of Ge(IV) for solutions containing 5 µM of catechin, 5 µM of alizarin sodium monosulfonate or 5 µM of alizarin complexone. Examined solution: 50 µM Ge(IV), 0.1 M acetate buffer (pH = 4.24). The HMDE electrode served as the working electrode.

Other factors that can potentially contribute to the increase of the AdSV signal of Ge(IV), such as the addition of an excess of ligand to shift the equilibrium of the reaction toward the complexed form of Ge(IV) or the prolongation of accumulation, did not provide any changes since the experiments were performed under the condition of saturation of the electrode surface. In this way, the influence of other variables was minimized and the obtained results confirmed that the presence of V(IV)-HEDTA does not affect the accumulation but does change the electrode process.

Another argument for the catalytic nature of the electrode process is the asymptotic shift of the peak potential towards the same value of the peak potential with increasing V(IV)-HEDTA concentration. This trend indicates that, regardless of the ligand complexing Ge(IV), the same process is responsible for the amplification of the observed signals, namely the reduction of V(IV) in the form of mixed complex comprising Ge(IV) catechol derivatives and V(IV)-HEDTA, as given by Scheme 5. The catalytic nature of the electrode process was also confirmed by CV voltammograms (Figure 14) showing that both negative and positive CV scans were cathodic, peak shaped, and corresponded to the reduction process given by Scheme 5. The shape of the backward scans developed in solutions containing Ge(IV)-catechin, Ge(IV)-alizarin monosulfonate, or Ge(IV)-alizarin complexone, accompanied by V(IV)-HEDTA, implies that the investigated catalytic systems may be attributed to catalytic systems of the second kind.

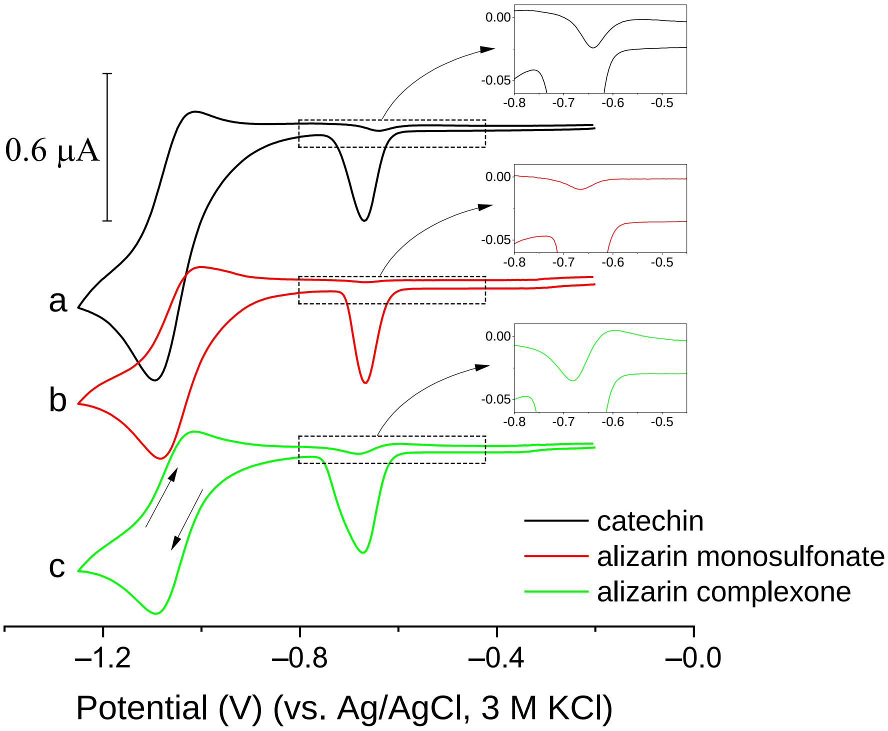

Figure 14. Cyclic voltammograms recorded in 0.1 M acetate buffer containing: (a) 5 μM of catechin, (b) 5 μM of alizarin sodium monosulfonate or 5 μM of alizarin complexone (c) and 50 μM of Ge(IV), 0.8 mM of V(IV), 1.6 mM of HEDTA. Scan rate 50 mVs^{-1}. The HMDE electrode served as the working electrode.

The dependence of the Ge(IV) peak current on its concentration was examined for new ligands under identical chemical and instrumental conditions. The concentration of ligands was 500 times lower than that recommended earlier for catalytic systems comprising catechol, pyrogallol, and chloranilic acid-based catalytic systems of Ge(IV). The large excess of ligand was not necessary to efficiently complex germanium, which is in contrast to procedures employing ligands, such as catechol, pyrogallol, and chloranilic acid. Additionally, it was noticed that the free ligand molecules may hinder the development of Ge(IV) catalytic signals by the competitive adsorption on the electrode surface. This phenomenon was observed for alizarin monosulfonate solutions. When the concentration of alizarin monosulfonate exceeded 0.5 mM, a decrease in the germanium peak was observed. When the concentration of alizarin monosulfonate reached a value of 1 mM, the germanium catalytic signal was no longer observed. To avoid problems related to the competitive adsorption of free ligands, solutions comprising 2 μM of catechin, alizarin monosulfonate, or alizarin complexone were applied. The examination of the dependence of the Ge(IV) peak current on its concentration started from the solution containing 0.04 μM Ge(IV), for which all the tested catalytic systems provided measurable signals but with different sensitivity (Figure 15a–c). The most beneficial signal, characterized by the highest S/N ratio, was provided by alizarin monosulfonate, and the smallest for alizarin complexone with catechin in the middle. Complete calibration curves are shown in Figure 15d.

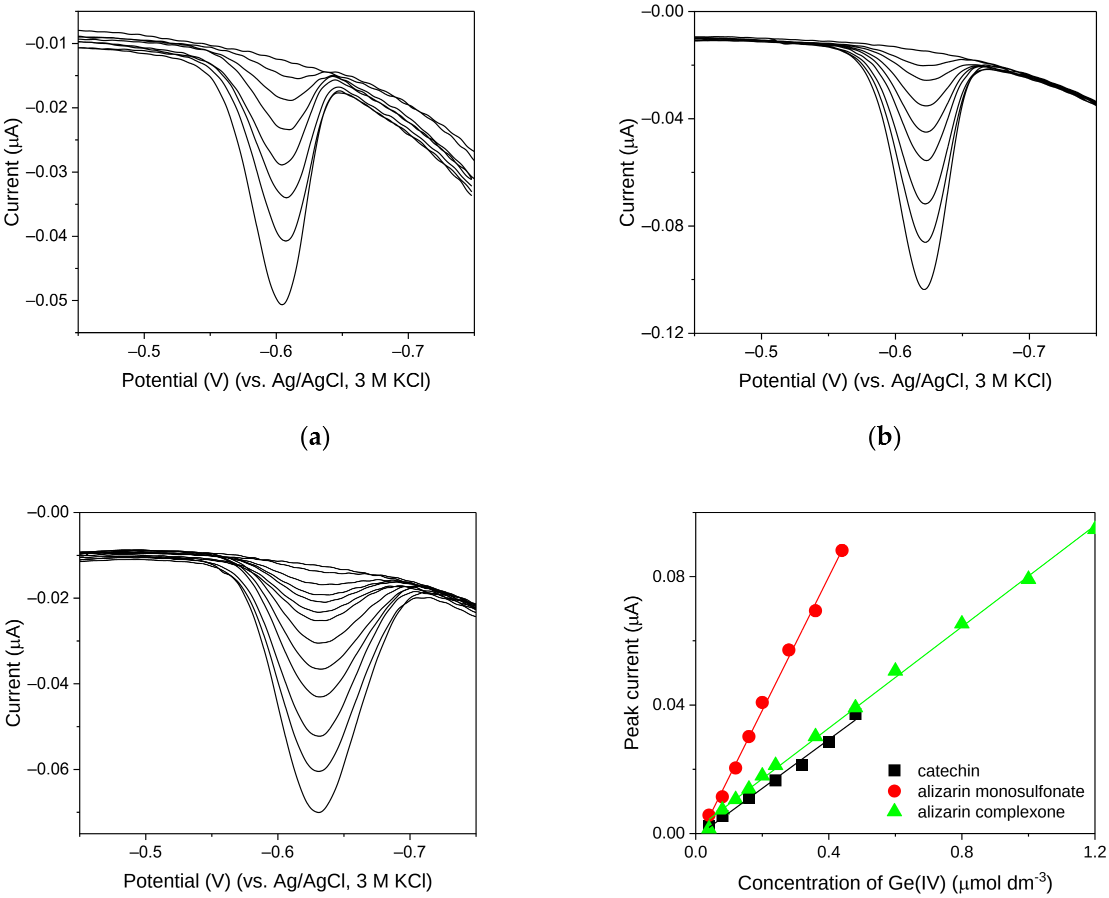

(**a**) (**b**)

(**c**) (**d**)

Figure 15. DP catalytic voltammetric curves of germanium with increasing Ge(IV) concentration ranging from (**a**) 0.04 µM to 0.48 µM of Ge(IV), (**b**) 0.04 µM to 0.52 µM of Ge(IV) and (**c**) 0.04 µM to 1.20 µM of Ge(IV), recorded using HMDE in the presence of (**a**) 2 µM of catechin, (**b**) 2 µM of alizarin sodium monosulfonate, and (**c**) 2 µM of alizarin complexone, 0.8 mM of V(IV), 1.6 mM of HEDTA and 0.1 M acetate buffer (pH = 4.24). The corresponding calibration plots are shown in panel (**d**). Instrumental parameters: $E_{acc} = -0.2$ V, $t_{acc} = 30$ s.

To accurately assess the analytical performance of the new catalytic systems, extensive research on the influence of numerous chemical and instrumental variables should be undertaken.

3. Conclusions and Prospects

The data reviewed here highlight the advantages of applying vanadium complexes used as catalysts that enhance the voltammetric signals of germanium. The vanadium-based catalytic systems are not only very efficient, offering amplification factors as high as 100, but also do not damage the sensing layer of the film electrodes and screen-printed supports, unlike other oxidants, such as nitrite, nitrate, bromate, and chlorate.

Although several papers offer reasonable explanations of the catalytic activity of different reagents toward Ge(IV), we decided to characterize the reaction mechanism in greater detail to better understand the origin of the differences in the reactivity of vanadium(IV) aminopolycarboxylic complexes. A starting point for the elucidation of the catalytic mechanism was the extraordinary ability of both V(IV) and Ge(IV) ions to form complexes with numerous ligands, as briefly described in the introduction section. The possibility of the formation of mixed, multinuclear bridged complexes was also reported and indirectly proven via voltammetric and spectrophotometric studies [42]. In conclusion, the most probable explanation for the amplification of Ge(IV) voltammetric signals entails the following:

1. The reduction of Ge(IV)-catechol (or ligands comprising a catechol moiety) to a very active Ge(II)-catechol complex.
2. The formation of a composite complex by Ge(II)-catechol and V(IV)-HEDTA (or other aminopolycarboxylic complexes).
3. The facilitated reduction of vanadium(IV) ions, a consequence of the binding of V(IV) to the Ge(II)-catechol-V(IV)-HEDTA complex.
4. The dissociation of the composite complex and detachment of Ge(II)-catechol ready to bind the subsequent V(IV)-HEDTA ion.
5. Facilitated reduction of newly bound vanadium(IV) ions and the formation of the catalytic cycle.

The effect of this reduction-complexation cycle is the amplification of the measured signal of germanium described in Scheme 5.

This review focused on the four most common aminopolycarboxylic complexes. However, there are many other chelating agents [50] that might be utilized in a similar way to HEDTA or EDTA vanadium complexes. To select those complexes that offer the best catalytic activity, a simple cyclic voltammetric test may be performed. A vanadium complex that undergoes a more electrochemically reversible reduction can amplify the germanium signal to a greater extent than one that is reduced irreversibly (see Figure 12b,c). Considering the continuous need for very sensitive, reliable, and robust analytical procedures of trace metal determination and an abundance of aminopolycarboxylic-based chelating agents, much remains to be discovered in the field of catalytic stripping voltammetry employing vanadium-based reagents.

Author Contributions: Conceptualization, A.K. and A.B.; writing—original draft preparation, A.K.; writing—review, A.B. and J.Z.; visualization, A.K. All authors have read and agreed to the published version of the manuscript.

Funding: This work was supported from the subsidy of the Ministry of Education and Science for the AGH University of Science and Technology in Kraków (Project No 16.16.160.557).

Institutional Review Board Statement: Not applicable.

Informed Consent Statement: Not applicable.

Data Availability Statement: The data are available on request from the author, (A.K.).

Conflicts of Interest: The authors declare no conflict of interest.

References

1. Treviño, S.; Díaz, A.; Sánchez-Lara, E.; Sanchez-Gaytan, B.L.; Perez-Aguilar, J.M.; González-Vergara, E. Vanadium in Biological Action: Chemical, Pharmacological Aspects, and Metabolic Implications in Diabetes Mellitus. *Biol. Trace Element Res.* **2019**, *188*, 68–98. [CrossRef]
2. Haber, J. Fifty years of my romance with vanadium oxide catalysts. *Catal. Today* **2009**, *142*, 100–113. [CrossRef]
3. Langeslay, R.R.; Kaphan, D.M.; Marshall, C.L.; Stair, P.C.; Sattelberger, A.P.; Delferro, M. Catalytic Applications of Vanadium: A Mechanistic Perspective. *Chem. Rev.* **2019**, *119*, 2128–2191. [CrossRef] [PubMed]
4. Israel, Y.; Meites, L. Vanadium. In *Encyclopedia of Electrochemistry of the Elements*; Bard, A.J., Ed.; Marcel Dekker Inc.: New York, NY, USA, 1976; Volume 7, pp. 336–378.
5. Shaw, M.J. Vanadium Electrochemistry. In *Encyclopedia of Electrochemistry*; Wiley: Hoboken, NJ, USA, 2006; pp. 357–381.
6. Galloni, P.; Conte, V.; Floris, B. A journey into the electrochemistry of vanadium compounds. *Coord. Chem. Rev.* **2015**, *301–302*, 240–299. [CrossRef]
7. Krakowiak, J.; Lundberg, D.; Persson, I. A Coordination Chemistry Study of Hydrated and Solvated Cationic Vanadium Ions in Oxidation States +III, +IV, and +V in Solution and Solid State. *Inorg. Chem.* **2012**, *51*, 9598–9609. [CrossRef] [PubMed]
8. Grant, A.W. Vanadium for high school students. *J. Chem. Educ.* **1977**, *54*, 500. [CrossRef]
9. Skyllas-Kazacos, M.; McCann, J. Vanadium redox flow batteries (VRBs) for medium- and large-scale energy storage. In *Advances in Batteries for Medium and Large-Scale Energy Storage*; Woodhead Publishing: Shaston, UK, 2015; pp. 329–386.
10. Pessoa, J.C. Thirty years through vanadium chemistry. *J. Inorg. Biochem.* **2015**, *147*, 4–24. [CrossRef]

11. León, I.E.; Díez, P.; Etcheverry, S.B.; Fuentes, M. Deciphering the effect of an oxovanadium(iv) complex with the flavonoid chrysin (VOChrys) on intracellular cell signalling pathways in an osteosarcoma cell line. *Metallomics* **2016**, *8*, 739–749. [CrossRef] [PubMed]
12. D'Cruz, O.J.; Uckun, F.M. Metvan: A novel oxovanadium(IV) complex with broad spectrum anticancer activity. *Expert Opin. Investig. Drugs* **2002**, *11*, 1829–1836. [CrossRef]
13. Del Carpio, E.; Hernández, L.; Ciangherotti, C.; Coa, V.V.; Jiménez, L.; Lubes, V.; Lubes, G. Vanadium: History, chemistry, interactions with α-amino acids and potential therapeutic applications. *Coord. Chem. Rev.* **2018**, *372*, 117–140. [CrossRef] [PubMed]
14. Alberico, E.; Micera, G.; Sanna, D.; Dessì, A. Coordination of oxovanadium(IV) to aminocarboxylic acids in aqueous solution. *Polyhedron* **1994**, *13*, 1763–1771. [CrossRef]
15. Wu, X.; Peters, B.J.; Rithner, C.D.; Crans, D.C. Multinuclear NMR studies of aqueous vanadium–HEDTA complexes. *Polyhedron* **2016**, *114*, 325–332. [CrossRef]
16. Li, H.-Y.; Li, D.-Q.; Yang, Y.; Zhang, X.; Diao, J.; Xie, B. Re-examination of complexation behaviors of V(v) and V(iv): Experimental investigation and theoretical simulation. *J. Anal. At. Spectrom.* **2020**, *35*, 878–885. [CrossRef]
17. Li, X.; Zhang, Z.; Liu, B.; Mu, W.; Yang, Y.; Martin, L.R.; Luo, S.; Rao, L. Complexation of Light Trivalent Lanthanides with N-(2-Hydroxyethyl)ethylenediamine-N,N′,N′-triacetic Acid in Aqueous Solutions: Thermodynamic Analysis and Coordination Modes. *Inorg. Chem.* **2019**, *58*, 15618–15628. [CrossRef] [PubMed]
18. Nash, K.L. The Chemistry of TALSPEAK: A Review of the Science. *Solvent Extr. Ion Exch.* **2015**, *33*, 1–55. [CrossRef]
19. Kanamori, K. Structures and properties of multinuclear vanadium(III) complexes: Seeking a clue to understand the role of vanadium(III) in ascidians. *Coord. Chem. Rev.* **2003**, *237*, 147–161. [CrossRef]
20. Leelavathy, L.; Anbu, S.; Kandaswamy, M.; Karthikeyan, N.; Mohan, N. Synthesis and characterization of a new series of unsymmetrical macrocyclic binuclear vanadyl(IV) complexes: Electrochemical, antimicrobial, DNA binding and cleavage studies. *Polyhedron* **2009**, *28*, 903–910. [CrossRef]
21. Pokrovski, G.S.; Martin, F.; Hazemann, J.-L.; Schott, J. An X-ray absorption fine structure spectroscopy study of germanium-organic ligand complexes in aqueous solution. *Chem. Geol.* **2000**, *163*, 151–165. [CrossRef]
22. Schleich, C.; Henze, C. Trace analysis of germanium. Part 2. Polarographic behaviour and determination by adsorptive strip-ping voltammetry, Fresenius. *J. Anal Chem.* **1990**, *338*, 145–148.
23. Piech, R. Study on simultaneous measurements of trace gallium(III) and germanium(IV) by adsorptive stripping voltammetry using mercury film electrode. *J. Appl. Electrochem.* **2010**, *41*, 207–214. [CrossRef]
24. Ly, S.Y.; Song, S.S.; Kim, S.K.; Jung, Y.S.; Lee, C.H. Determination of Ge(IV) in rice in a mercury-coated glassy carbon electrode in the presence of catechol. *Food Chem.* **2006**, *95*, 337–343. [CrossRef]
25. Alvarez, J.M.; Calzon, J.G.; Fonseca, J.L. Electrochemical Reduction of Ge(IV) Catalyzed by o-Catechol at the Dropping Mercury Electrode and at the Hanging Mercury Drop Electrode after Adsorptive Preconcentration. *Electroanalysis* **1999**, *11*, 656–659. [CrossRef]
26. Alvarez, J.L.M.; Calzón, J.A.G.; Fonseca, J.M.L. Square-wave voltammetry of the o-catechol-Ge(IV) catalytic system after adsorptive preconcentration at a hanging mercury drop electrode. *Talanta* **2001**, *53*, 721–731. [CrossRef]
27. Hasebe, K.; Hikima, S.; Kakizaki, T.; Iwashimizu, T.; Aoki, K. Trace determination of germanium by means of adsorption waves in differential-pulse polarography. *Analyst* **1990**, *115*, 413–416. [CrossRef]
28. Sun, C.; Gao, Q.; Liu, L. Adsorptive stripping measurements of germanium(IV) in the presence of pyrogallol. *Talanta* **1995**, *42*, 881–884. [CrossRef]
29. Aguilar, J.C.; de Gyves, J. Determination of germanium(IV) in sulphide ores by differential pulse polarography in pyrogal-lol-sulfuric acid media. *Anal. Chim. Acta* **1995**, *306*, 243–247. [CrossRef]
30. Gökmeşe, F.; Gökmeşe, E.; Osman Solak, A. A new adsorptive square-wave stripping voltammetric method for the trace anal-ysis of germanium, Hacettepe. *J. Biol. Chem.* **2008**, *36*, 215–221.
31. Bond, A.M.; Kratsis, S.; Newman, O.M.G. Adsorptive Stripping Voltammetric Determination of Germanium in Zinc Plant Electrolyte. *Electroanalysis* **1998**, *10*, 387–392. [CrossRef]
32. Grabarczyk, M. Optimization of Adsorptive Stripping Voltammetry Procedure Using Chloranilic Acid as a Complexing Agent for the Determination of Ultra-Trace Germanium in Natural Water Samples. *J. Electrochem. Soc.* **2017**, *164*, H872–H876. [CrossRef]
33. Grabarczyk, M.; Adamczyk, M. Bismuth film electrode and chloranilic acid as a new alternative for simple, fast and sensitive Ge(iv) quantification by adsorptive stripping voltammetry. *RSC Adv.* **2018**, *8*, 15215–15221. [CrossRef]
34. Canham, R.G.; Aikens, D.A.; Winograd, N.; Mazepa, G. Mechanism of polarographic reduction of germanium(IV) in acidic catechol medium. *J. Phys. Chem.* **1970**, *74*, 1082–1087. [CrossRef]
35. Jinhui, S.; Kui, J. Adsorptive complex catalytic polarographic determination of germanium in soils and vegetables. *Anal. Chim. Acta* **1995**, *309*, 103–109. [CrossRef]
36. Zhong, S.; Su, J.; Chen, L.; Tong, J.; Jia, W.; Li, X.; Zou, H. Determination of Total Germanium in Chinese Herbal Remedies by Square-Wave Catalytic Adsorptive Cathodic Stripping Voltammetry at an Improved Bismuth Film Electrode. *Int. J. Electrochem.* **2013**, *2013*, 735019. [CrossRef]
37. Li, Y.-H.; Chen, X.-H.; Huang, M.-H.; Zhou, F.-Q. Catalytic Adsorptive Stripping Voltammetry of Germanium(IV) in the Presence of Gallic Acid and Vanadium(IV)-EDTA. *Electroanalysis* **2007**, *19*, 704–708. [CrossRef]

38. Zhang, Y.; Wu, Y. Enhancement Mechanism of the Oscillopolarographic Current of Germanium(IV)-Trihydroxybenzoic Acid System and Application. *Anal. Sci.* **1997**, *13*, 279–284. [CrossRef]
39. Muniz Alvarez, J.L.; Garcia Calzon, J.A.; Lopez Fonseca, J.M. Coupling of Ligand-Catalyzed Electroreduction of Metal Ions with Redox Electrocatalysis. Application of the o-Catechol-Ge(IV)-V(IV) Double Catalytic System for the Sensitive Determi-nation of o-Catechol. *Electroanalysis* **2001**, *13*, 181–185. [CrossRef]
40. Zarębski, J.; Bobrowski, A.; Gonciarczyk, J.; Królicka, A. Extremely sensitive germanium stripping voltammetric determination with the use of a new Ge(IV)-catechol-V(IV)-HEDTA catalytic adsorptive system. *Electrochim. Acta* **2019**, *324*, 134859. [CrossRef]
41. Królicka, A.; Zarębski, J.; Bobrowski, A. Catalytic Adsorptive Stripping Voltammetric Determination of Germanium Employing the Oxidizing Properties of V(IV)-HEDTA Complex and Bismuth-Modified Carbon-Based Electrodes. *Membranes* **2021**, *11*, 524. [CrossRef] [PubMed]
42. Zarębski, J.; Bobrowski, A.; Gonciarczyk, J.; Królicka, A. Selection of Optimal Ligand and Vanadium(IV) Complexonate for Sensitive Catalytic Adsorptive Stripping Voltammetric Quantification of Germanium. *Electroanalysis* **2020**, *32*, 2213–2219. [CrossRef]
43. Zarębski, J.; Bobrowski, A.; Królicka, A.; Gonciarczyk, J.; Manolopoulou, V.; Economou, A. A novel catalytic adsorptive stripping voltammetric method for the determination of germanium ultratraces in the presence of chloranilic acid and the V(IV)·HEDTA complex. *J. Solid State Electrochem.* **2020**, *24*, 2891–2899. [CrossRef]
44. Sun, C.; Gao, Q.; Xi, J.; Xu, H. Determination of germanium(IV) by catalytic cathodic stripping voltammetry. *Anal. Chim. Acta* **1995**, *309*, 89–93. [CrossRef]
45. Bobrowski, A.; Zarębski, J. Catalytic systems in adsorptive stripping voltammetry. *Electroanalysis* **2000**, *12*, 1177–1186. [CrossRef]
46. Bobrowski, A.; Zarebski, J. Application of catalytic adsorptive stripping voltammetry in water analysis. *Water Sci. Technol. Water Supply* **2001**, *1*, 1–8. [CrossRef]
47. Bobrowski, A.; Zarebski, J. Catalytic Adsorptive Stripping Voltammetry at Film Electrodes. *Curr. Anal. Chem.* **2008**, *4*, 191–201. [CrossRef]
48. Mirčeski, V.; Bobrowski, A.; Zarebski, J.; Spasovski, F. Electrocatalysis of the first and second kind: Theoretical and experimental study in conditions of square-wave voltammetry. *Electrochimica Acta* **2010**, *55*, 8696–8703. [CrossRef]
49. Bobrowski, A.; Królicka, A.; Śliwa, J.; Zarębski, J.; Januś, M.; Kyzioł, K. PVD fabrication of lead film electrodes and their catalytic adsorptive stripping voltammetric performance in the presence of oxidants. *Electrochem. Commun.* **2018**, *94*, 49–54. [CrossRef]
50. Nowack, B.; VanBriesen, J.M. Chelating Agents in the Environment. In *Active Learning in General Chemistry: Specific Interventions*; American Chemical Society (ACS): Washington, DC, USA, 2005; pp. 1–18.